Oct 22nd, 12:00 AM

Experimental Techniques for Plate Buckling

W. Pennington Vann

John Sehested

EXPERIMENTAL TECHNIQUES FOR PLATE BUCKLING

by

W. Pennington Vann* and John Sehested**

INTRODUCTION

When a plate element is very thin and is subjected to in-plane compression or shear, its buckling behavior may be important. In recent years considerable progress has been made in developing numerical techniques for the evaluation of plate buckling loads. However, few new concepts have been advanced for use in plate buckling experiments. Such experiments are important in verifying numerical data and in relating these data to the buckling and post-buckling of real plates. This is especially true for plates with odd shapes and uncertain boundary conditions, even though most of the reported tests have been conducted on simple rectangular plates.

In this paper several buckling concepts are reviewed, amplified and combined with a view toward gaining more useful and reliable information from plate stability experiments. Particular attention is devoted to accounting for imperfections and other factors in arriving at the average in-plane buckling stress, N_{cr}. N_{cr} is the bifurcation stress for a perfectly flat plate which corresponds to the real, imperfect plate actually tested. The principles discussed are interpreted graphically and are illustrated with data from actual experiments. Only elastic behavior is considered.

---

*Associate Professor of Civil Engineering, Texas Tech University, Lubbock, Texas.

**Project Engineer, Brown and Root, Inc., Houston, Texas.

REVIEW OF BASIC BEHAVIOR

Consider a rectangular plate loaded in compression along opposite edges, as shown in Fig. 1. The curves in the figure represent the relationship between the average edge stress, N, and the lateral deflection, w_p, at some point P on the surface of the plate. Plots of the same general type are obtained for any plate, regardless of its dimensions or boundary conditions. The curves shown differ only according to the initial out-of-plane deflection and the theory employed in the analysis.

The horizontal line (a) in Fig. 1 represents non-zero lateral deflections which would be obtained if the plate were perfectly flat and linear strain-displacement theory were valid in all ranges of deflection. This is the behavior assumed in finding the critical stress by an eigenvalue analysis, except that only infinitesimal lateral deflections are considered. In such an analysis the bifurcation stress, N_{cr}, is the primary quantity of interest, and the magnitude of the deflection at N_{cr} is indeterminate.

Using the same linear theory for a plate with some initial lateral deflection, w_{po}, at point P, the deflection from the reference plane varies as shown by curve (b). At low stresses this curve can have a less regular shape than is shown, but it must approach line (a) asymptotically as w_p approaches infinity. In principle, the asymptotic ordinate will give the same value of N_{cr} as an eigenvalue solution for the corresponding perfectly flat plate. Curves (a) and (b) are equally representative of the behavior of an elastic column.

Curve (c) in Fig. 1 represents the load-deflection relationship obtained for a perfectly flat plate when post-buckling effects are taken into account. If the buckling shape is maintained in the early stages of post-buckling, this curve has a parabolic form,

$$\frac{N}{N_{cr}} = 1 + c\left(\frac{w_p}{h}\right)^2 \qquad (1)$$

where c is a constant and h is the thickness or the plate. For example, it can be shown using the analysis of Ref. 9 that for a square plate with simple supports all around and in-plane deflection prevented along the two lateral edges, the constant c is 0.872.

Finally, curve (d) in Fig. 1 gives the load-deflection behavior of an imperfect plate when post-buckling effects are taken into account. Except when unusual imperfection patterns occur, this is the actual behavior for an arbitrary point on a real elastic plate. Curve (d) may be thought of qualitatively as the summation of curve (b) -- the linear-theory part -- and the difference between curve (c) and N_{cr} -- the non-linear or post-buckling part. Since the first of these component curves has a negative curvature, while the second has a positive curvature, curve (d) must have an inflection point.

In view of the behavior indicated by curve (d), it is not surprising that there is no single, clear-cut definition of the "buckling load" of a real (imperfect) plate. As will be discussed below, a variety of buckling criteria have been proposed, and each one can produce a different buckling value for the same plate under identical loading conditions. In the present work the buckling values obtained by the different criteria are compared with respect to the single quantity, N_{cr}, which is clearly defined as the bifurcation stress of the associated perfectly flat plate. N_{cr} is very useful in analysing and predicting post-buckling behavior. However, with regard to design, considerations such as peak strains and waving amplitudes are also very important, and N_{cr} may not be the only quantity of interest.

Before leaving Fig. 1 the reader should recall that the same four types of curves may be drawn for a column in compression, but that post-buckling effects are not significant for a column until much larger lateral deflections are attained. This is because the column has no tension field action like that which affects a plate at relatively small deflections. Accordingly, curve (c) rises much more gradually for a column, and curve (d) is close to curve (b) until the latter is almost horizontal. Stated differently, for a column the linear theory is applicable over a much larger range of deflections.

TYPES OF PLATE BUCKLING MEASUREMENTS

The most traditional instrumentation used in plate buckling experiments measures the lateral or out-of-plane deflection at one or more points on the surface of the plate. Dial gages or LVDT's may be used for this purpose, providing a plot of the type shown by curve (d) in Fig. 1. Adequate sensitivity is easily attained with such standard instruments, except for rather small plates (say less than two inches in width or less than .01 inch in thickness). Note that the data obtained do not include the deflection with respect to the reference plane prior to loading (that is, the initial imperfection, w_{Po}).

A second very popular type of instrumentation consists of electrical resistance strain gages which are paired on opposite surfaces at one or more locations about the plate. Usually it is easier to place a number of these gage pairs than to mount many dial gages on a specimen. From each gage pair one can determine average (i.e., mid-plane) strains and differential (i.e., bending) strains. Strain measurements have the advantage that they can be compared directly to yield strains, but they cannot be correlated easily with deflections.

A typical set of data obtained from a pair of strain gages during a buckling experiment is shown in Fig. 2. At low loads the two compressive strains are essentially equal, and they increase linearly with load. At higher loads the curves begin to spread apart due to bending induced by inevitable eccentricities. The larger the eccentricity, the wider the spread between the curves. As the buckling load is approached, the bending of the plate increases significantly, causing the strain on the convex side to reach a maximum compressive value, after which it decreases. Meanwhile, the strain on the concave side becomes quite large, due to the addition of in-plane and bending effects.

Other types of instrumentation, including photoelastic techniques, are feasible for plate buckling, but they have not been used extensively. Therefore, attention will be focused on buckling criteria which are associated with lateral deflection and surface strain measurements.

BUCKLING CRITERIA ASSOCIATED WITH LATERAL DEFLECTIONS

Southwell Plot. - For a column, the most powerful method for determining the experimental buckling load is to plot the load and deflection data in a form called a Southwell plot (8), rather than in the form of Fig. 1. In a Southwell plot, w/P (deflection over load) is indicated on the ordinate and w is shown on the abscissa. If the pattern of initial imperfections has the shape of the fundamental buckling mode, it may be shown that this plot will be a straight line having an inverse slope equal to the critical load, P_{cr}. Moreover, any real pattern of initial imperfections may be expanded into an infinite series in terms of the buckling modes, and in the corresponding series for deflection under axial loading, the fundamental term rapidly becomes dominant as the axial load increases. Because of the influence of higher mode terms,

experimental data do not fall on a straight line at low loads, but they do form a straight line at higher loads. In addition to the critical load, the amplitude of the fundamental component of the initial lateral deflection may be determined from the plot.

It is important to note that linear beam-column theory is used in this approach, and that by using linear theory for a plate the same basic relationship can be developed fo find N_{cr}(9). In graphical terms, this means that curve (b) is Fig. 1 corresponds to a straight line when its points are replotted in Southwell coordinates. However, as discussed above, the true curve (d) deviates from curve (b) at a much earlier stage for a plate than for a column, and this causes the Southwell plot to deviate from a straight line. In fact, it was recognized long ago (2) that for a plate the Southwell plot cannot be counted upon to give an accurate value of N_{cr}.

Nevertheless, the Southwell method can be attempted with plate buckling data, simply by finding the closest approximation to a straight line on the Southwell plot. At loads in the vicinity of N_{cr} and higher, the Southwell plot line will definitely not be straight, just as the shape of curve (d) in Fig. 1 is much different from that of curve (b) in this range, due to post-buckling effects. This range is not needed, however, since the buckling load need not be approached closely. At very low loads there is always scatter in the Southwell points because of the influence of higher mode terms, so this range should not be used either. A useful straight line can only emerge in the intermediate region, say between $0.3N_{cr}$ and $0.7N_{cr}$, where curves (b) and (d) of Fig. 1 tend to be similar in shape. The key to finding a useful straight line is for the higher mode terms to become negligible before post-buckling effects become too large.

It should be noted that the value of N_{cr} from a Southwell plot for a plate will always be too high, and that the accuracy will be better for a smaller amplitude of the fundamental component of the initial imperfection. These trends hold true because post-buckling effects always cause curve (d) to lie above curve (b) in Fig. 1, the difference being larger for larger imperfections. N_{cr} from the Southwell plot corresponds to extrapolating the early portion of curve (d) as a rectangular hyperbola out to a horizontal asymptote. The farther curve (d) lies above curve (b), the higher the level of the asymptote.

Top-of-the-Knee. - Some years ago a less mathematical but somewhat more pragmatic method was used to estimate the buckling load of a plate from load-deflection data. The method was based upon the fact that in many cases an experimental curve (type (d) in Fig. 1) has a very straight transition region which contrasts with the negative-curvature "knee" at the lower end. The load at the top of this knee, i.e., at the beginning of the transition region, was taken as the buckling load (1). This method has advantages in its simplicity and in the physical interpretation of "buckling" as loss of stiffness: The top of the knee may be thought of as representing the minimum slope on the load-deflection diagram. On the other hand, the method has disadvantages in that the top of the knee is often difficult to pinpoint, and the selected value is invariably lower than N_{cr}. It has been shown (2), that the error tends to increase as the imperfection amplitude decreases.

Inflection Point. - A method closely related to the top-of-the-knee method is one which takes as the buckling value the load at the inflection point of curve (d), (5). In the sense that this point is truly the point of minimum slope, the inflection point should coincide with the top of the knee. However, the inflection point has the distinction of being defined mathematically. This allows analytic techniques to be used, such as fitting

a parabola to the data by least squares, and then finding the inflection point of the parabola (6). In practice both the top of the knee and the inflection point are difficult to establish accurately since the transition region spreads gradually over a fairly wide range of loads. The inflection point normally comes out higher, simply because it is regarded as lying somewhere in the middle of the transition region, rather than at its beginning.

Illustrative Example. - The three approaches just presented are illustrated in Fig. 3, which gives dial gage data from two plate tests carried out by Schlack (5,6). The curves in part (a) are of the form of Fig. 1, and the corresponding Southwell plots are given below in part (b). Also shown are the properties of the specimens. Schlack used the parabola-fitting technique to obtain the values of N_{cr} shown for the inflection point method, while the top-of-the-knee values were selected by the authors. The theoretical buckling values were also given by Schlack, based on the measured specimen properties.

The expected lower bound trends are found for the top-of-the-knee method. The inflection point method gives higher values, but still below the theoretical values. As yet, no analytical study has been presented concerning the accuracy of the inflection point method. The curves in part (a) are good examples of the difficulty in locating the top of the knee and the inflection point. These specimens were carefully selected to minimize the initial imperfections, and yet the changes in shape are very gradual. Specimen (2) has a smaller initial deflection, since the first slope of curve 2 is steeper, and the curvature reversal is slightly more evident for that specimen.

It can be seen that neither Southwell plot in part (b) of Fig. 3 is a straight line. A fairly straight segment seems to appear for specimen 1,

but any slope chosen for either specimen must involve considerable guesswork. The slopes that are shown result in values of N_{cr} which are much larger than the theoretical values, indicating that the method is quite inaccurate for these plates. This inaccuracy may be related to the amplitude of the imperfection. The fundamental component of the imperfection appears to be of the order of 0.4h for specimen 2 and 0.7h for specimen 1, but in each case a steeper slope (in agreement with the theorectical N_{cr}) would produce a small imperfection. As expected, the Southwell plot value is less accurate for the specimen with the larger imperfection.

Summary. - Of the three lateral deflection techniques discussed, the inflection point method appears to give the best value of N_{cr}. A value found by the top-of-the-knee method may fall close to the inflection point value, but it generally is too low and it may be harder to identify. The Southwell plot method has the merit of giving an upper bound, but the bound is likely to be so inaccurate that it is of little practical value.

Other load-deflection methods have also been used in plate buckling experiments,and there is always close agreement if the initial imperfections are very small. In such cases the choice of method is unimportant. However, carefully manufactured and selected laboratory specimens are not generally representative of products used in practice. For practical applications the imperfections have a strong influence on the behavior, and an understanding of the buckling criterion is important.

BUCKLING CRITERIA ASSOCIATED WITH STRAIN MEASUREMENTS

Maximum Surface Strain. - The buckling criterion that is most often used when surface strains are measured is the maximum surface strain or "strain reversal" criterion (4). Here the critical load corresponds to a

maximum strain on the convex side of the plate (point A in Fig. 2). This load is well-defined, but the maximum surface strain method has long been recognized as giving a buckling value lower than N_{cr}. As with the methods previously considered, the deviation from N_{cr} increases with increasing initial imperfections (2).

Maximum Membrane Strain. - In another strain criterion, the load corresponding to the maximum mid-plane strain is chosen as the critical load (3). This mid-plane or "membrane" strain is the average of the strains measured by two gages which are paired on opposite sides of the plate. The method is somewhat less sensitive than other methods, and also is less general. This is because at a particular location in a plate with particular boundary conditions, the mid-plane strain may or may not reach a maximum value at buckling (12). For example, a maximum normally is attained in the center of a rectangular plate, but along one side the longitudinal strain tends to increase, rather than decrease, after buckling. Therefore, this method is not recommended in cases in which the distribution of in-plane strains is either complex or unknown. Wang and Winter (10) found that the maximum membrane strain is generally higher than the maximum surface strain.

Southwell Plot for Strains. - Using linear theory, one can develop a Southwell Plot which relates the average or mid-plane strain measured by a pair of gages on opposite faces to the differential or bending strain recorded by the same two gages (7). Since linear behavior is inherently assumed in applying the Southwell method, such a plot has the same range of validity as a Southwell plot for deflections. As before, the associated critical stress is too high, exceeding N_{cr} by a larger amount for larger initial imperfections. An important advantage of the

method is that it allows a single system of instrumentation to provide an upperbound value of N_{cr} as well as the lower bound value obtainable by the maximum surface strain method. The spread between these bounds then gives a measure of the accuracy. Another advantage of the Southwell approach is that the elastic buckling strain can be estimated even when it is above the yield strain of the material.

USE OF SEVERAL STRAIN MEASUREMENTS

So far plate buckling techniques have been discussed only for an individual measurement such as might be provided by a dial gage or a pair of strain gages at a particular point on a plate. The question then arises as to what correlation there might be in the same experiment between the results from different measurements. This is of particular interest in view of the fact that initial imperfections tend to affect the measured critical stress. Such imperfections vary in an unknown, irregular way over the surface of an actual plate.

Figure 4 illustrates the use of a number of strain gage pairs in measuring the buckling of the web of a channel (7). The testing arrangement shown in part (a) is of the type often used in the past (11). Twelve pairs of electrical resistance strain gages were mounted on the surfaces of the web, as shown in part (b) of the figure. Strains measured at gage points Ib, IIb and IIIb are plotted in Fig. 5 versus the average edge stress, N. The maximum surface strain criterion gives values of N_{cr} of 940 and 970 lb/in for points Ib and IIb, respectively, but no maximum strain was reached at gage point IIIb. In this test the loading was not increased further because yielding was incipient at the tension flanges of the specimen. It is clear, nevertheless, that N_{cr} measured at point IIIb would have been about 1,160 lb/in.

In analyzing these difference, it is instructive to estimate the waveform of the buckled web. The signs and amplitudes of the various strains, together with visual and dial gage observations, indicated a waveform close to that of Fig. 4c. Apparently section III was rather close to a nodal line, causing smaller bending strains to develop at point IIIB than at the other two points.

At sections I and II the data from gage lines "a" and "c" gave slightly higher values of N_{cr} than the data from gage line "b", according to the maximum surface strain criterion. This would appear to agree with the conclusion drawn earlier, that in this method a larger imperfection amplitude results in a smaller value of N_{cr}. At a given section the largest initial deflection would be expected to occur at the center of the web.

In Fig. 6 are shown strain-type Southwell plots which were generated by the data of Fig. 5. Corresponding values of N_{cr} are shown in Table A. As expected, the values of N_{cr} thus obtained are all larger than those found by the maximum surface strain criterion. At gage point IB the two criteria give values of N_{cr} which differ by 23%, but at gage point IIb the difference is only 15%. Since the mean N_{cr} between the two methods is 1066 lb/in at point Ib and 1048 lb/in at point IIb, the results are quite consistent. The bound concepts discussed above indicate a smaller initial deflection at IIb, as do the relevant strain and Southwell plots.

At sections I and II, similar results were obtained from all of the gage pairs used. However, at section III all three gage pairs indicated very large values of N_{cr} when determined by the Southwell method. This is related to the fact that the straight line appearing in Fig. 6c is less well defined than the others and is generated entirely by stresses

close to N_{cr}. Since post-buckling effects are quite strong in this range, the resulting value of N_{cr} is inaccurate. Once again, the proximity of section III to a nodal line has seriously affected the results. This shows that a single data point may not be reliable, and that several values of N_{cr} should not be averaged blindly, but rather scrutinized very carefully.

In order to study imperfection effects further, the specimen of Fig. 4 was tested twice more after being shifted along its length with the support and load points remaining stationary. Each shift of the specimen was equal to the measured flat width of the web, b. The results indicated a strong influence of the imperfections in determining the buckling pattern, but a rather small change in N_{cr}.

It may be noted, finally, that theoretical values (9) of the buckling stress for this particular plate are 808 lb/in for simply supported lateral edges (k=4.0) and 1,410 lb/in for built-in lateral edges (k=6.98). Using an intermediate value of the buckling coefficient, k=5.27, as suggested in Ref. 10, N_{cr} is equal to 1,063 lb/in. The latter value is in close agreement with the averages cited above.

CONCLUSIONS

With the possible exception of the inflection point method, all of the methods considered for evaluating N_{cr} experimentally tend to decrease in accuracy as the imperfection amplitude increases. The results presented show that the inflection point method is the best of the techniques associated with lateral deflection measurements, and that the maximum surface strain and the Southwell plot techniques can be combined effectively for measurements of surface strain. The Southwell plot always gives an

upper bound and appears to be much more useful for strains than for deflections.

In practical applications it is found desirable to compare and correlate data from various points over the surface of the plate. These data help to define the buckling shape as well as the pattern of imperfections, and clarify the measured buckling stresses.

ACKNOWLEDGEMENT

Part of this work was sponsored by NASA under grant NGL 44-066-033.

REFERENCES

1. Heimerl, G. J. and Roy, J. A., "Preliminary Report on Tests of 24S-t Aluminum-Alloy Columns of Z-, Channel, and H-Section That Develop Local Instability." NACA RB No. 3J27, 1943.

2. Hu, P. C., Lundquist, E. E. and Batdorf, S. B., "Effect of Small Deviations from Flatness on Effective Width and Buckling of Plates in Compression," NACA Technical Note No. 1124, September, 1946.

3. Jombock, J. R. and Clark, J. W., "Postbuckling Behavior of Flat Plates," Trans., ASCE, Vol. 127, Part II, 1962, p. 227.

4. Rossman, C. A., Bartone, L. M., and Dobrowski, C. V., "Compressive Strength of Flat Panels with Z-Section Stiffeners," NACA ARR No. 4B03, 1944.

5. Schlack, A. L., Jr., "Elastic Stability of Pierced Square Plates," Experimental Mechanics, Vol. 4, No. 6, June, 1964, pp. 167-172.

6. Schlack, A. L., Jr., "Experimental Critical Loads for Perforated Square Plates," Experimental Mechanics, Vol. 8, No. 2, Feb., 1968, pp. 69-74.

7. Sehested, J., "Experimental Buckling Criteria for Thin Pierced Plates," Master of Science Thesis, Rice University, Houston, Texas, 1971.

8. Southwell, R. V., "On the Analysis of Experimental Observations in Problems of Elastic Stability," Proc. Royal Soc. (London), Series A, Vol. 135, April, 1932, pp. 601-616.

9. Timoshenko, S. P. and Gere, J. M., Theory of Elastic Stability, Second Edition, McGraw-Hill, New York, 1961.

10. Wang, S. T. and Winter, G., "Cold-Rolled Austenitic Stainless Steel: Material Properties and Structural Performance, Cornell Report No. 334, Ithica, New York, July, 1969.

11. Winter, G., "Cold-Formed, Light-Gage Steel Construction," Journal of the Structural Div., ASCE, Vol. 85, No. ST9, Nov., 1959.

12. Yamaki, N., "Experiments on the Postbuckling Behavior of Square Plates Loaded in Edge Compression," Journal of Applied Mechanics, Trans. ASME, Vol. 83, Series E, June, 1961.

APPENDIX -- NOTATION

N, N_{cr} = average edge stress, corresponding critical value

P, P_{cr} = load, critical load on a column

b = flat width of rectangular plate

c = constant in Eq. 1

h = plate thickness

k = buckling coefficient

w_p, w_{po} = total, initial lateral deflection at general point

ν = Poisson's Ratio

a = length of rectangular plate

TABLE A. - Values of N_{cr} (in lb/in) for Channel Specimen of Fig. 4

Gage Point	Maximum Surface Strain Criterion	Southwell Plot for Strains
Ia	1,000	1,150
b	940	1,190
c	1,000	1,180
IIa	1,010	1,110
b	970	1,125
c	1,025	1,150
IIIa	-	1,460
b	(1,160)	1,485
c	-	1,470
IVb	970	1,150

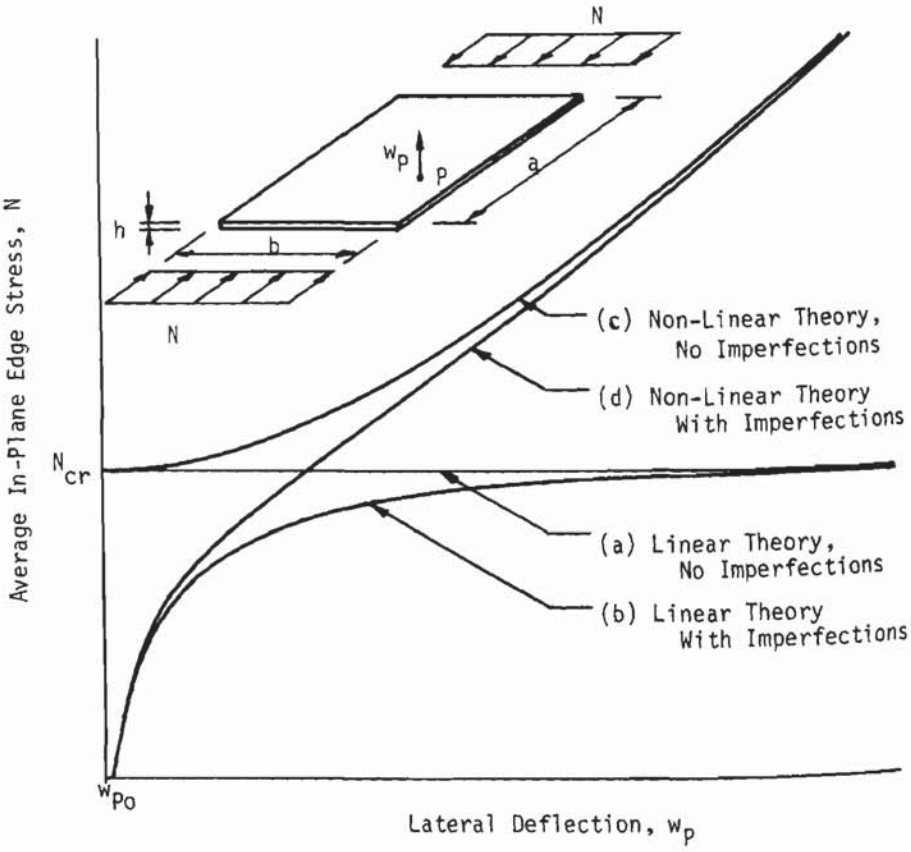

FIG. 1. TYPICAL RELATIONSHIPS BETWEEN EDGE STRESS AND LATERAL DEFLECTION

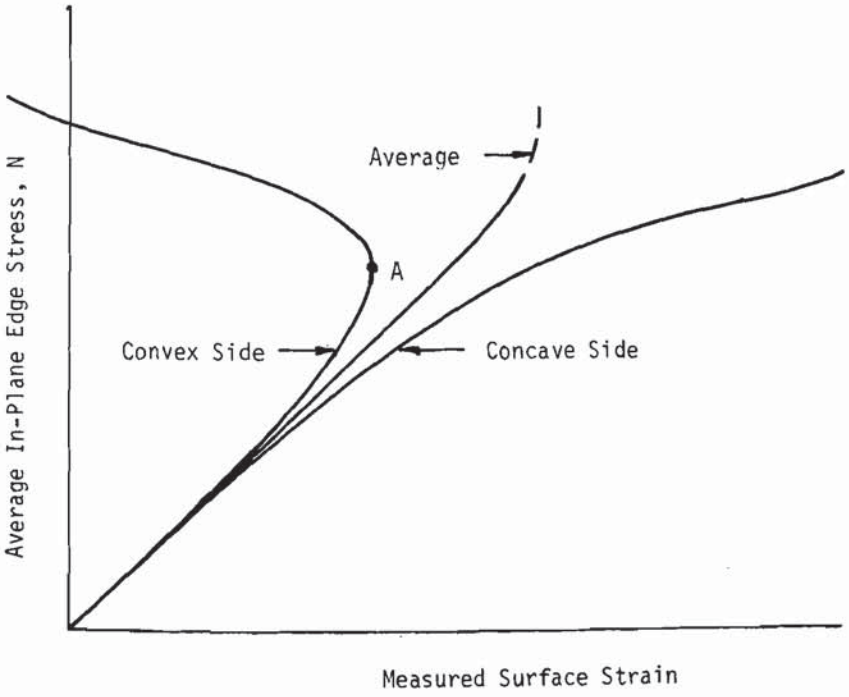

FIG. 2. TYPICAL RELATIONSHIPS BETWEEN EDGE STRESS AND PAIRED SURFACE STRAINS

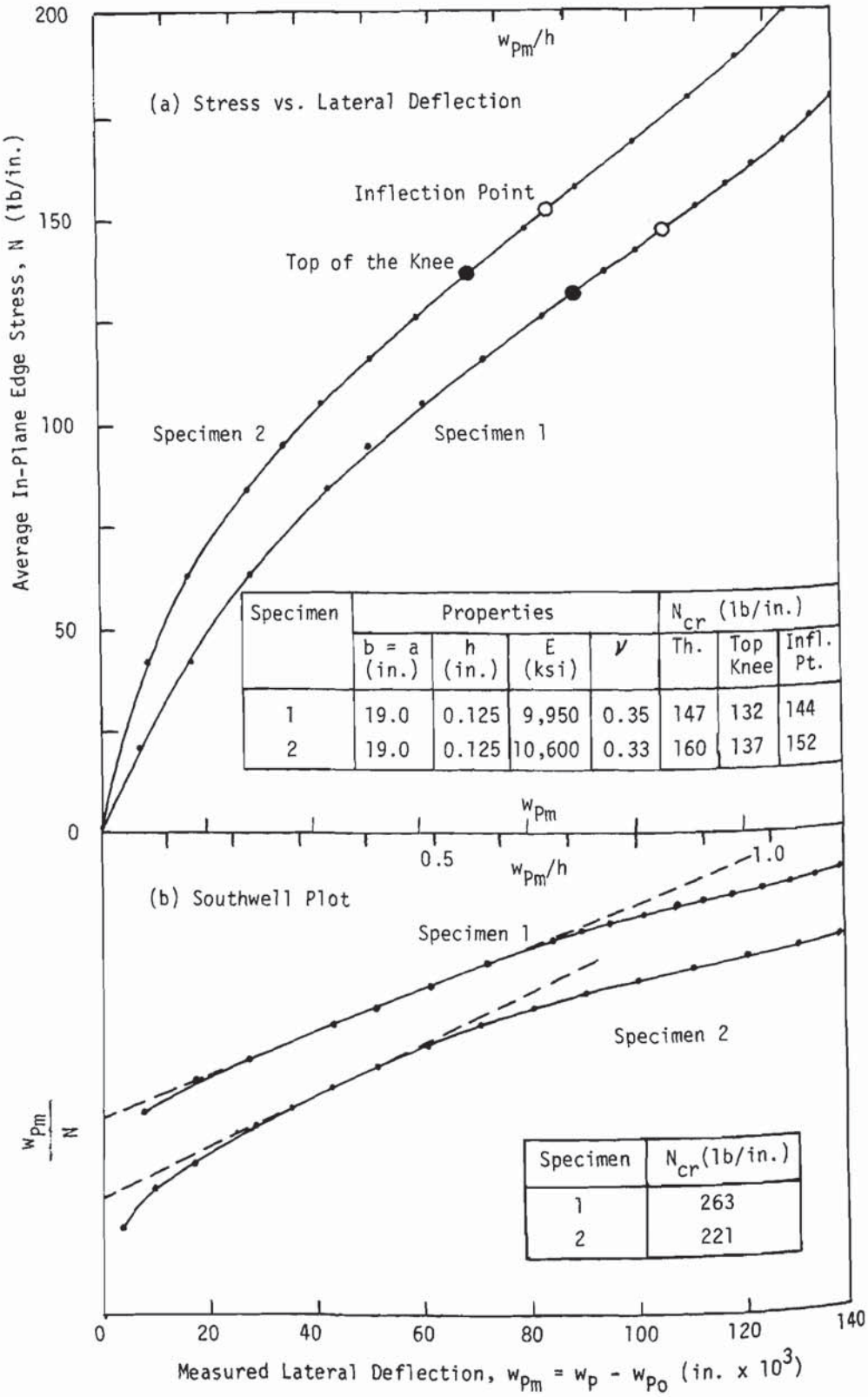

Specimen	Properties				N_{cr} (lb/in.)		
	b = a (in.)	h (in.)	E (ksi)	ν	Th.	Top Knee	Infl. Pt.
1	19.0	0.125	9,950	0.35	147	132	144
2	19.0	0.125	10,600	0.33	160	137	152

Specimen	N_{cr}(lb/in.)
1	263
2	221

FIG. 3. BUCKLING DATA OBTAINED BY SCHLACK (5,6)

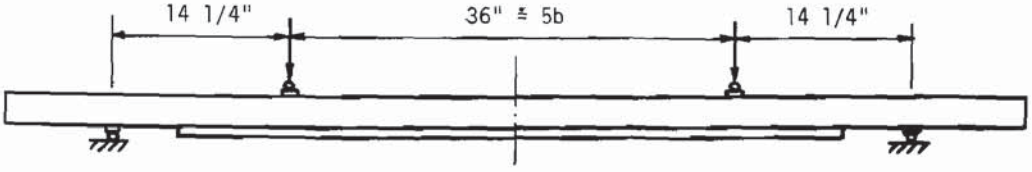

(a) Loading Arrangement (Side View)

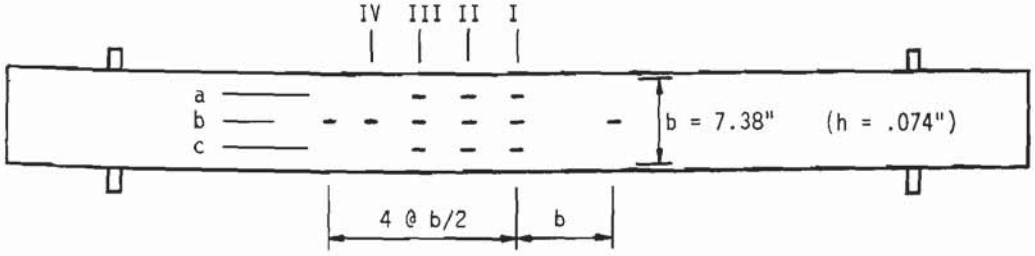

(b) Pattern of Paired Web Gages (Plan View)

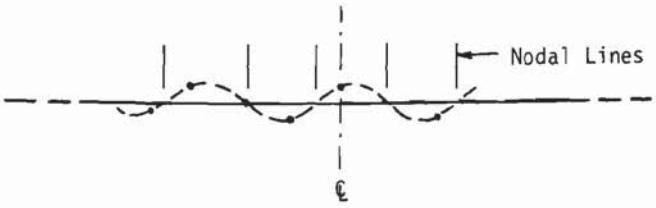

(c) Approximate Buckle Waveform

FIG. 4. CHANNEL SPECIMEN WITH WEB IN UNIFORM COMPRESSION (7)

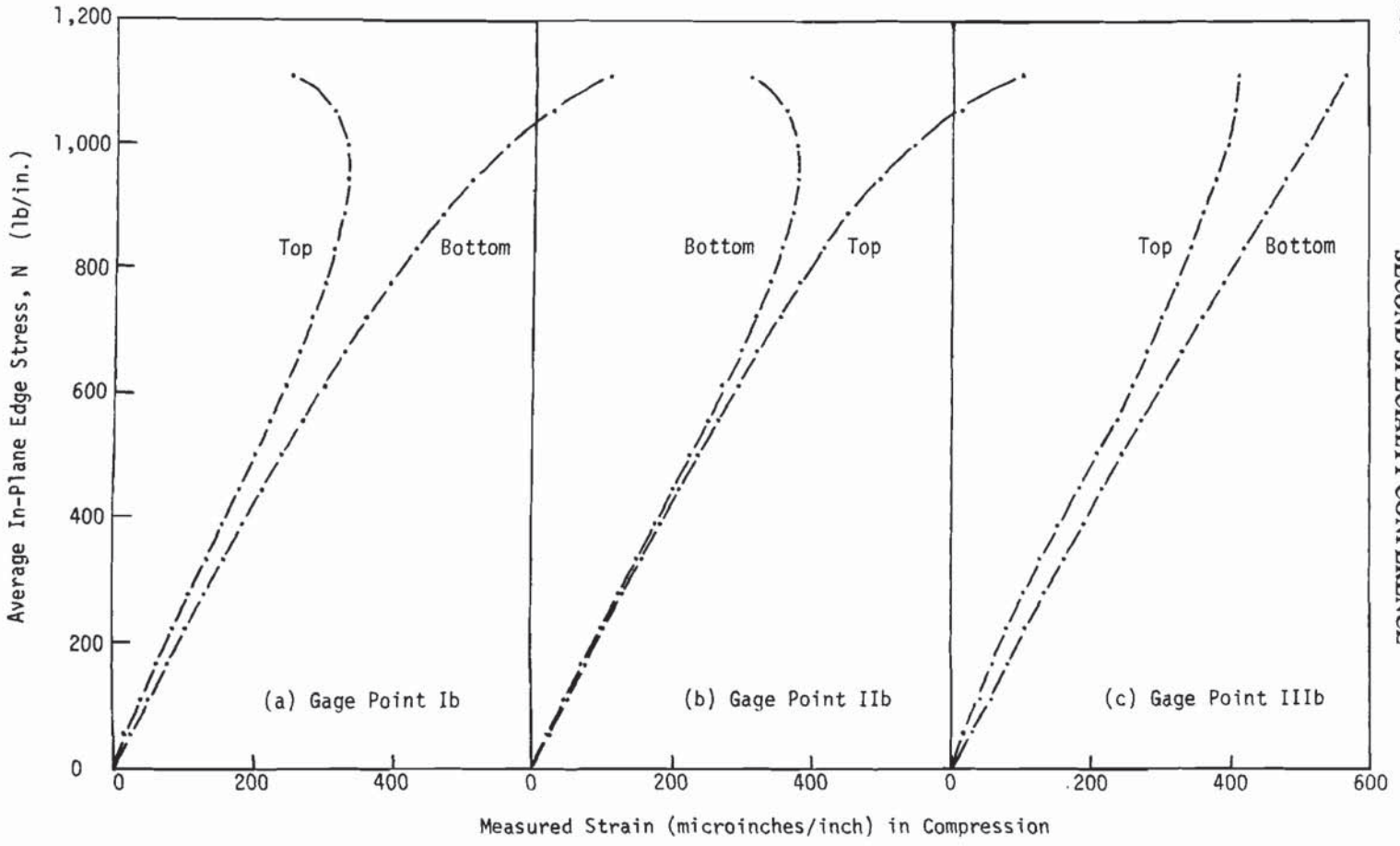

FIG. 5. SURFACE STRAINS MEASURED IN TEST OF CHANNEL SPECIMEN

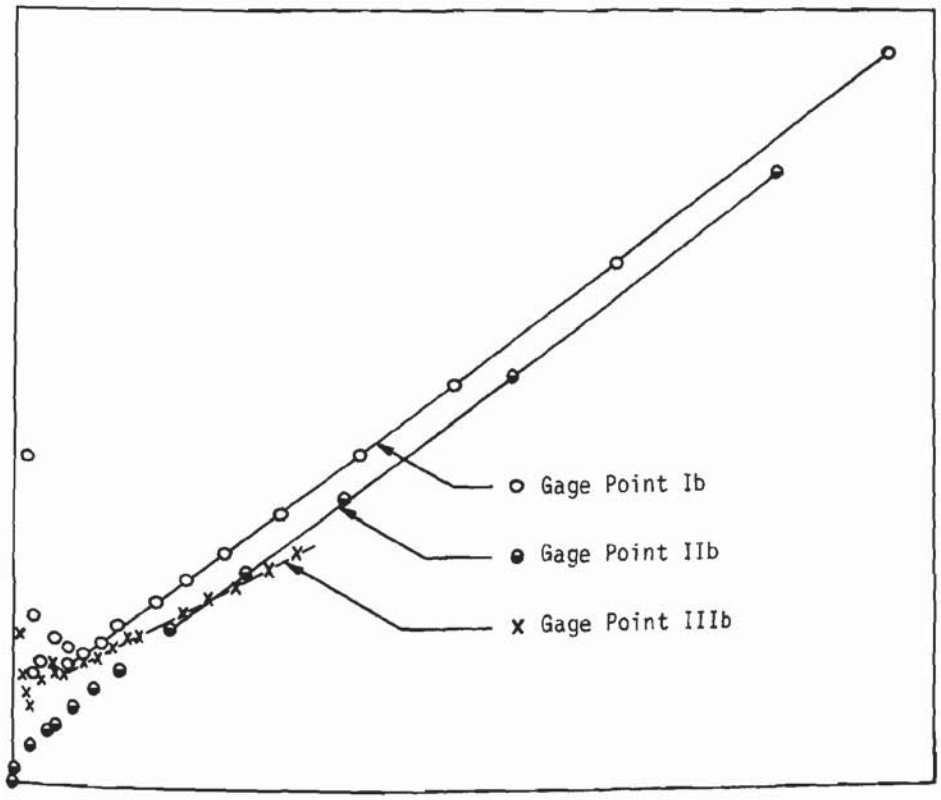

FIG. 6. SOUTHWELL PLOTS FOR STRAIN DATA OF FIG. 5